Omicron: Rapid Mesh Generation on HPC Platforms for the Study of Near Surface Phenomena with Remote Sensing

Owen J. Eslinger, Amanda M. Hines, Stacy Howington, Jerrell R. Ballard, Jr., John Peters, Barry C. White, and Preston McAllister
USACE Engineer Research and Development Center (ERDC), Vicksburg, MS
{owen.j.eslinger, amanda.m.hines, stacy.e.howington, jerrel.r.ballard, john.f.peters, barry.c.white, preston.b.mcallister}@erdc.usace.army.mil

Abstract

A technique is presented for rapidly producing unstructured finite element meshes in support of large-scale remote sensing simulations. These tetrahedral meshes typically have more than one million elements and more than 250 thousand nodes, and allow for arbitrary placement of objects into the domain. Open-source mesh generation packages are used in conjunction with a tetrahedra element smoothing operation to achieve the desired final meshes. Meshes can be reproduced in less than 30 minutes on a Cray XT3 architecture.

1. Introduction

As part of an ongoing effort to improve automated target recognition algorithms for remote sensing technologies, a suite of closely coupled numerical simulators has been developed. These models include high-resolution thermal and moisture transport finite element models, as well as solar (ray casting) and vegetation models. The resulting tightly coupled system allows heat transport simulations to be performed at a very fine scale. This setup is well suited for the testing of specific scenes with controlled environmental conditions, in particular meteorological and time-of-day conditions, which might otherwise be difficult and time consuming to reproduce in the field. However, this suite serves as a complement to, rather than a replacement for, field and laboratory testing of remote sensors.

These numerical simulations require the rapid and robust production of unstructured finite element meshes of the shallow subsurface for the moisture and thermal codes. The meshes need to include natural and man-made objects to achieve realism and relevancy, e.g., rocks and soda cans. This work will focus on the mesh generation process, which has been achieved by taking advantage of open-source (black-box) mesh generation software. The tetrahedra that are output are then post-processed with a mesh smoothing technique to ensure quality elements in the final tetrahedral mesh. In addition, the process allows for the inserted objects to be arbitrarily placed, i.e., buried, flush with or protruding from the ground surface. A simple mesh repair operation around the objects is utilized to avoid poorly shaped tetrahedra in these regions. When desired, subsurface soil regions can be assigned as a post-process step. This ability extends to statistically generated soil distributions using site-specific information obtained from soil samples.

2. Countermine Computational Testbed

Collectively, the numerical simulators and their pre- and post-processing tools are called the Countermine Computational Testbed. The purpose of the testbed is to represent the thermal, hydrological, and meteorological processes that contribute significantly to the infrared response of typical scenes. The testbed must produce visually realistic images, which requires spatial variability at a resolution that is the same or better than that measurable by the fielded sensor (about 2–4 cm).

2.1. Scene Generation

A typical scene includes soils, rocks, plants, and targets or other objects. The soil volume normally extends 0.5 to 1 m into the ground and includes a detailed representation of the ground surface. Surface texture dictates the spatial variability in surface temperatures, especially at low sun angles and with sparse vegetation. Spatial distribution of soil materials also contributes to temperature variability. High variability tends to make target discrimination more difficult.

For thermal infrared scene modeling, the vegetative elements on the surface may be represented by either a

0-7695-3088-5/07 $25.00 © 2007 IEEE

plane parallel abstraction or as individual three-dimensional geometric models. Because of the sensor ground resolution requirements, the plants are modeled as individual geometric objects where the stems and leaves are described as triangular facets. Geo-typical representations of the plants are based on in situ measurements. Thermal conduction in plant materials is relatively small and the thermal analysis of the plants can be computed independently of the ground model. Thus, the plants are not an integral part of the finite element mesh but are merely placed on the surface mesh.

2.2. Terrain Physics Models

Energy is introduced to the scene by a ray casting model. The ray caster uses the sun position, a discrete representation of the hemispherical sky, and hourly meteorological data to compute inbound radiation distributed among six spectral bands. These loadings are applied to individual soil, vegetation, rock, and target facets in the scene. The ray caster includes shading of facets by other facets and permits partial transmission of energy through plant facets. Facets reflect a portion of the energy within each spectral band. The vegetation model accepts the energy input from the ray caster and computes leaf temperatures based on material properties, air temperature, wind speed, etc. In addition to plant facet temperatures, the vegetation model estimates stomatal resistance and the resulting water demand from its root system.

The soil moisture and thermal migration model (ADH)[8,10] is a finite element model that uses linear basis functions on tetrahedra. The model approximates Richards equation for partially saturated groundwater flow and heat conduction and convection with moisture-content-dependent properties. ADH accepts rainfall from the meteorological data and inbound energy from the ray caster as some of its boundary conditions. Heat flux at the ground surface also depends on sensible and latent heat exchange. Mesh refinement and coarsening can be triggered by multiphysics error indicators. The mesh refinement scheme attempts to retain the original element aspect ratio by splitting oldest edges first. The model accommodates parallel processing with dynamic load balancing.

The product of the vegetation and soil models is predicted temperature at each of the nodes for the time step. The ray caster uses these nodal temperatures to compute emitted energy, which is added to the reflected energy and projected to an idealized, near-ground image plane. An atmospheric model samples the near-ground image and simulates transmission effects to the height of the sensor. A sensor model simulates the effects of optical blur and sensor noise. The resulting synthetic sensor image may be used as if collected from the field to test and improve automated target recognition algorithms.

3. Mesh Generation Method

The tetrahedral meshes used for the moisture and heat transport models are generated using software that takes advantage of the packages Triangle[11-13] and TetGen [7,14,15] which are both compiled as callable libraries. This mesh generation process has been simplified to rapidly produce meshes for remote sensing simulations within the Countermine Computational Testbed. The meshes can be reproduced quickly, reducing the need to store large numbers of large mesh files. This easy production of meshes also greatly reduces the overall time needed to run simulations.

The product of the mesh generation method described in this work is a full, conforming, three-dimensional (3D) tetrahedral mesh of the shallow subsurface region under investigation. There are no overset grids or hybrid elements. Objects are completely integrated into the mesh and are denoted with unique material identification (ID) for each tetrahedron. The plants are handled outside of this scheme. The top of the domain, which represents the ground surface, has a realistic topography based on Light Detection and Ranging (LIDAR) data. These data come in the form of (X,Y,Z) values and come from field measurements, although the data could be generated using geostatistics or by some other suitable method. Occasionally, the LIDAR data are incomplete due to "shadow" effects from plants or other obstacles. In this case, the holes are patched using information from the immediate region around the hole.

Constraints on the maximum tetrahedral volume and maximum area of surface triangles are supplied by the user at runtime.

The remainder of this section describes in detail the mesh generation steps in the order of operation.

3.1. Top Surface Mesh Generation

The surface of the domain, Figure 2, was generated using Shewchuk's Triangle code guided by the bounding region. After the flat mesh was produced, the heights, Z values, were assigned based either on LIDAR input data coming from field measurements or data generated based on geostatistical descriptors. The resolution of the LIDAR imagery is generally higher than required for the mesh generation. The LIDAR representation is coarsened to match the specified mesh resolution by a simple smoothing process. A simple averaging was used to determine relative heights of the surface nodes, as it appeared to form more realistic topographies than inverse distance weighting techniques. The radius of influence

used for this assignment was 3 cm, which was based upon the amount of available input data.

Triangle is guided by an upper constraint on the area of the triangles supplied by the user and a lower bound of 33 degrees for the minimum angle constraint when it is producing the initial flat mesh.

3.2. Mesh Remainder of Bounding Domain

The vertical sides of the domain and flat bottom are also meshed with Triangle, resulting in a closed domain. The same constraints on Triangle used for the top of the domain are again used for the remaining five sides. However, there is one additional constraint on the meshing of these flat surfaces. For each surface, no additional nodes are allowed to be placed on edges where nodes exist, i.e., the skeletal frame of the domain. This is needed so that the top, sides, and bottom may be aligned to form a closed bounding region, without hanging nodes.

Currently, only regions with a total of six sides are available. More general, polygonal regions are not considered.

3.3. Object Insertion, Mesh Repair

One of the most important aspects of this process is the need to include objects within the domain, e.g., rocks and land mines. This procedure is handled automatically. These objects will be fully integrated into the mesh and therefore are added prior to tetrahedralization. They may be arbitrarily placed and either buried, flush with, or protruding from the ground surface. They may not protrude from the sides or bottom of the domain. There is no hard limit on the number of objects that can be included. They may be imported as empty, faceted shells or may be complete tetrahedral meshes with multiple material regions within the object. Objects imported as shells are tetrahedralized by TetGen whereas full objects are treated as holes. In the latter case, the object tetrahedra are added back into the domain afterward.

Intersections between the objects and the surface of the domain are detected using TetGen. A simple repair operation is performed in the immediate neighborhood of each object when needed to "stitch" the object into the surface mesh. The mesh of the object is never altered but a "high water mark" is identified. That is, nodes on the object are separated into two groups: those completely above the surface mesh and all others. Intersecting triangles from the surface mesh are removed and the "apron" around the object is then remeshed using Triangle. This apron reconnects the surface mesh with the object shell along this "high water mark". In the process the surface mesh may be deformed slightly and/or nodes may be added. The object apron created by the reconnection process is not always visually detectable. Sensitivity analysis shows that element quality in the apron regions has no effect on the result of simulations nor degrades performance of the equation solvers.

3.4. Subsurface Mesh Generation

As stated before, the result of the previous steps is a closed domain with objects that is used as input to TetGen. The only guidance given to TetGen, other than the bounding region, is a volume constraint supplied by the user, closed material regions denoting the objects within the domain, and a request not to subdivide any input surface triangle. Experience has shown that using the quality constraints available in TetGen will dramatically increase the time needed for mesh generation for this problem. Therefore, the quality constraint is disabled in TetGen and the smoothing of the resulting tetrahedra is handled as a post-process step.

3.5. Tetrahedral Mesh Smoothing

Because the mesh quality constraints are disabled in TetGen for this work, there is no implied or explicit guarantee on element quality. As a final step then, the output mesh is post-processed with a mesh-smoothing algorithm to ensure quality tetrahedra in the final mesh. In this smoothing procedure, the internal nodes of the domain may be moved; however, the connectivity of the elements is not altered. The smoothing process employs the element quality metric and element size metric detailed in References 1 and 2. The shape metric has been shown to be equivalent to other tetrahedron quality metrics, as it correctly identifies all types of poorly shaped elements, i.e., "sliver" elements, "needle" elements, "flat" elements, etc. In general, "flat" elements tend to appear in this process more often than all of the other types of poorly formed elements combined. There were few of these, and they tended to be near the top surface of the domain. Linking the variable topography of the surface to the relatively regular sides and bottom of the domain most likely caused these malformed elements during the Delaunay mesh generation process.

The size metric quantifies the difference between the size of a given element and some optimum size. The average element volume is used throughout the domain as the optimum in this work.

A variety of optimization techniques have been employed in the smoothing step. Primarily, the steepest descent and Broyden-Fletcher-Goldfarb-Shanno algorithms were used for the optimization problem and were implemented as described in Reference 9. The gradients of the objective function are derived and computed explicitly. Generally, a static number of

iterations (50) are taken, with a goal of improving the final mesh as opposed to meeting a target quality constraint.

3.6. Identifying Subsurface Soil Regions

Subsoil regions can be assigned as a post-process step when desired. A distribution of soil regions can be derived using site-specific geostatistical information, i.e., borehole data, and the program T-PROGS[3-6]. The output of T-PROGS is a Cartesian grid with material IDs distributed according to variogramgenerated Markov chains. The program HYSSOP[16] creates smoothed boundaries between the subsoil material regions using a string-of-pearls constraint-based smoothing algorithm. Each tetrahedron in the mesh is assigned a material ID using its centroid to determine its encompassing material region.

3.7. SceneGen Modeler

A scene development GUI (graphical user interface) has also been developed in support of the Countermine Computational Testbed. The purpose of this modeler is to orient and visualize the input data prior to tetrahedralization. SceneGen allows the user to visualize the LIDAR data, supplied bounding region, and object shells at their relative locations. It also allows visualization of vegetation and other energy occluding objects used in the ray caster and vegetation models. This ability to view all of the objects in the scene simultaneously allows the user to plan and verify the scene carefully. Other capabilities of the modeler include the ability to move and orient the objects within the scene. The modeler can then output the newly edited scene in formats for mesh generation and ray casting.

A screen shot of the SceneGen modeler can be seen in Figure 5. In this scene both plants and objects are being moved within the scene prior to mesh generation.

4. Results

All tetrahedral meshes shown in this paper were created using a single core on one processor on a Cray XT3 architecture with 2 GB of memory. In addition to the Cray XT3 architecture, this automated mesh generator package has also been built on the SGI Origin 3900 as well as desktop machines running Linux and Mac OS X. However, it is currently executed most often on the Cray XT3 architecture because of the speed and amount of available memory of this machine. It can be run on the front or back end of the XT3.

At present at least seven users of varying educational backgrounds are creating meshes. Over the past year, these seven users have created approximately 50 meshes that have been used in hundreds of heat transport simulations. Because the typical user needs to change only the number and (X,Y,Z) locations of objects, the time needed for training new users is generally well under an hour.

The total time needed to create the mesh in Figure 1 was less than one hour, most of which was spent in the planning of object locations. There are approximately 1.5 million tetrahedral elements and 270 thousand nodes. The total 'computational time was nine minutes with the majority of that time spent in the mesh, smoothing out the step (approximately 3–4 minutes). In this manner, the objects could be moved (or others could be added) and the new mesh could be generated in well under an hour. Therefore, the testing of new scenarios with a similar configuration can be achieved with minimal effort.

The surface of the domain is shown in Figure 2. This surface had 57 thousand triangles prior to the insertion of objects, and the resulting topography can clearly be seen in the figure. There are a total of four rocks in the final domain, which can be seen in the full mesh in Figure 1. The colors are determined by material type. A closer view of two of the rocks can be seen in Figure 3. The object intersection routines have seamlessly integrated the rocks into the scene.

A separate mesh was created using roughly the same area, and the result of a full simulation can be seen in Figure 4. In this figure the colors correspond to temperatures and there is preferential loading in the direction of the sun, with shadows being cast by the objects. This demonstrates the interactions of the solar model with the vegetation model and the heat transport model in the shallow subsurface.

5. Future Work

Large field scale (1 km × 1 km) simulations are being planned for the near future. The meshing approach described in this paper is near the memory limitations of a single processor on the Cray XT3 being used. Initially, larger domains will be created in a patchwork fashion with matching vertical boundaries between the subdomains. Simple scalability will be achieved by using a separate processor for each subdomain.

Currently, tetrahedral element volume is determined by the resolution needed on the surface of the domain. However, the resulting number of tetrahedra is quite large. The number of elements produced could be reduced by grading the mesh in the negative z-direction, especially below the depth of diurnal temperature fluctuations.

6. Conclusion

The process of rapid, unstructured tetrahedral mesh generation for remote sensing simulations has been achieved on a variety of computational architectures. The final mesh can include multiple objects, each at an arbitrary location within the domain and the mesh generally can be reproduced in much less than an hour. Individual scenes can be planned in detail, allowing objects to be carefully placed, thereby greatly increasing the number of scenarios that can be tested.

Acknowledgements

This work has been funded by the Common High Performance Computing Software Support Initiative Institute for Maneuverability and Terrain Physics Simulation under the direction of Dr. David Horner at the US Army Engineer Research and Development Center in Vicksburg, MS.

References

1. Branets, L., "A variational grid optimization method based on a local cell quality metric." Ph.D. Thesis, The University of Texas at Austin, 2005.

2. Branets, L. and G.F. Carey, "A local cell quality metric and variational grid smoothing algorithm." *Proceedings of the 12th International Meshing Roundtable*, Santa Fe, NM, USA, pp. 371–378, 2003.

3. Carle, S.F., *T–PROGS: Transition Probability Geostatistical Software*, University of California, Davis, 1999.

4. Carle, S.F. and G.E. Fogg, "Modeling spatial variability with one and multidimensional continuous-lag Markov chains." *Math. Geol.*, 29(7), pp. 891–917, 1996.

5. Carle, S.F. and G.E. Fogg, "Transition probability-based indicator geostatistics." *Math. Geol.*, 28(4), pp. 453–476, 1996.

6. Deutsch, C.V. and A.G. Journel, *GSLIB: Geostatistical Software Library and User's Guide,* New York: Oxford University Press, 1998.

7. Edelsbrunner, H. and N.R. Shah, "Incremental topological flipping works for regular triangulations." *Algorithmica*, vol. 15, pp. 223–241, 1996.

8. Howington, S.E., R.C. Berger, J.P. Hallberg, J.F. Peters, A.K. Stagg, E.W. Jenkins, and C.T. Kelley, "A model to simulate the interaction between groundwater and surface water." *Proceedings of the 1999 High–Performance Computing Users' Group Meeting*, Monterey, CA, USA, Washington, DC, DoD HPC Modernization Office, 1999.

9. Kelley, C.T., "Iterative Methods for Optimization, Frontiers of Applied Mathematics." vol. 18, Philadelphia: SIAM, 1999.

10. Schmidt, J.H., "A 3-D Adaptive finite element method for transport processes." Master's Thesis, The University of Texas at Austin, 1995.

11. Shewchuk, J.R., "Adaptive precision floating–point arithmetic and robust geometric predicates." *Discrete & Computational Geometry*, vol. 18, no. 3, pp. 305–363, 1997.

12. Shewchuk, J.R., "Delaunay refinement algorithms for triangular mesh generation." *Computational Geometry: Theory and Applications*, vol. 22, no. 1–3, pp. 21–74, 2002.

13. Shewchuk, J.R., "Triangle: Engineering a 2D quality mesh generator and Delaunay triangulator." in *Applied Computational Geometry: Towards Geometric Engineering*, Ming C. Lin and Dinesh Manocha, Eds., Volume 1148 of Lecture Notes in Computer Science, pp. 203–222, Berlin, Springer–Verlag, May 1996.

14. Si, H., "On Refinement of Constrained Delaunay Tetrahedralizations." *Proceedings of the 15th International Meshing Roundtable*, Birmingham, AL, USA, pp. 509–528, 2006.

15. Si, H. and K. Gaertner, "Meshing piecewise linear complexes by constrained Delaunay tetrahedralizations." *Proceedings of the 14th International Meshing Roundtable*, San Diego, CA, USA, pp. 147–163, 2005.

16. White, B. and O.J. Eslinger, "Modeling Subsurface Phenomena for Tetrahedral Meshes." *Proceedings of the 2006 HPCMP Users' Group Conference*, Denver, CO, pp. 212–215, June 2006.

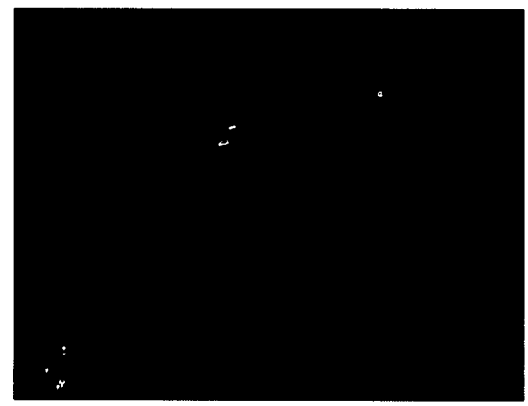

Figure 1. The full 3D mesh with 272k nodes and 1.5M tetrahedra shown prior to the addition of plants

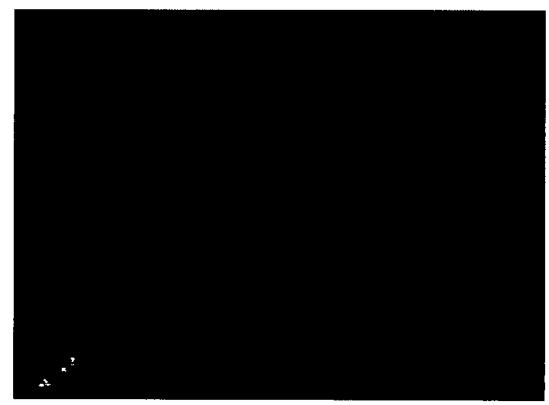

Figure 2. Surface mesh, prior to object insertion, with 57,201 triangles covering a square domain, 10 meters on a side

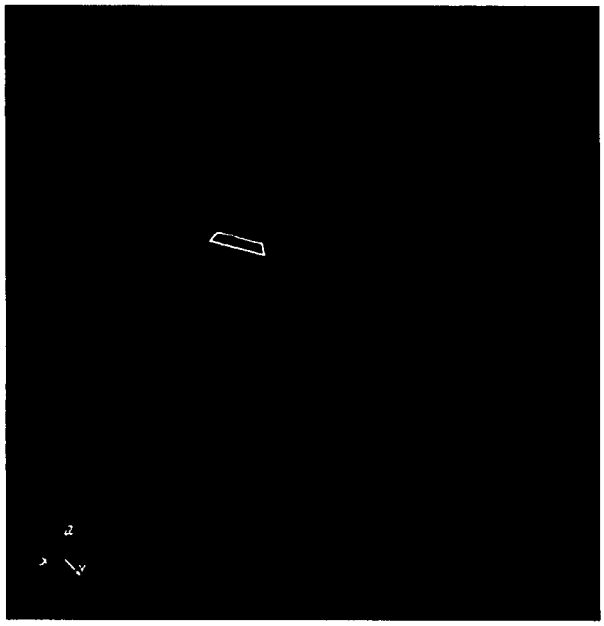

Figure 3. Close-up of two rocks. Notice that the aprons around the rocks are blending into the full mesh.

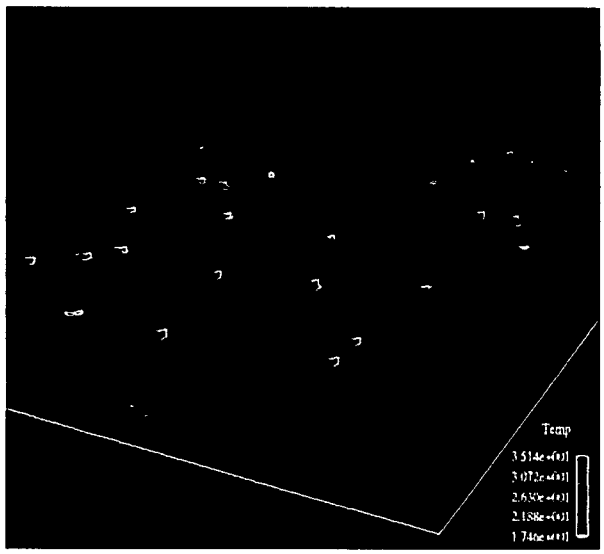

Figure 4. Region with many objects, two types of plants in various locations, and the resulting temperatures during the course of a simulation

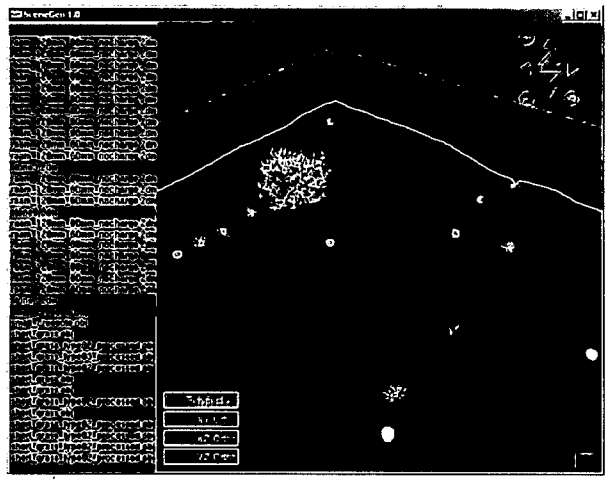

Figure 5. Screen Shot of SceneGen Modeler Software. In this figure, there are several objects as well as several plants being incorporated into the scene. The highlighted objects are in the process of being moved.

Figure 6. A view along the surface of a mesh with multiple plants and objects. Notice the rock in the scene which has been blended into the surface mesh.